Title Page

Title: Monitoring transmission intensity of trachoma with serology: a multi-country study

Authors: Christine Tedijanto[1], Anthony W. Solomon[2], Diana L. Martin[3], Scott D. Nash[4], Jeremy D. Keenan[1,5], Thomas M. Lietman[1,5,6,7], Patrick J. Lammie[8], Kristen Aiemjoy[9], Abdou Amza[10,11], Solomon Aragie[12], Ahmed M. Arzika[13], E. Kelly Callahan[4], Sydney Carolan[1], Adisu Abebe Dawed[14], E. Brook Goodhew[3], Sarah Gwyn[3], Jaouad Hammou[15], Boubacar Kadri[11], Khumbo Kalua[16], Ramatou Maliki[13], Beido Nassirou[11], Fikre Seife[17], Zerihun Tadesse[12], Sheila K. West[18], Dionna M. Wittberg[1], Taye Zeru[19], Benjamin F. Arnold[1,5] *

Author affiliations:

[1] Francis I. Proctor Foundation, University of California San Francisco, San Francisco, CA, USA, 94158
[2] Department of Control of Neglected Tropical Diseases, WHO, Geneva, Switzerland
[3] Division of Parasitic Diseases and Malaria, Centers for Disease Control and Prevention, Atlanta, GA, USA 30329
[4] The Carter Center, Atlanta, GA, USA, 30307
[5] Department of Ophthalmology, University of California San Francisco, San Francisco, CA, USA, 94158
[6] Institute for Global Health Sciences, University of California San Francisco, San Francisco, CA 94143
[7] Department of Epidemiology and Biostatistics, University of California San Francisco, San Francisco, CA 94143
[8] Neglected Tropical Diseases Support Center, Task Force for Global Health, Atlanta, GA, USA, 30030
[9] Division of Epidemiology, Department of Public Health Sciences, University of California Davis School of Medicine, Davis, CA, USA
[10] Programme FSS/Université Abdou Moumouni de Niamey, Programme National de Santé Oculaire, Niamey, Niger
[11] Programme National de Lutte Contre la Cecité, Niamey, Niger.
[12] The Carter Center Ethiopia, Addis Ababa, Ethiopia
[13] The Carter Center Niger, Niamey, Niger
[14] Amhara Regional Health Bureau, Bahir-Dar, Ethiopia
[15] Service of Ocular and Otological Diseases, Epidemiology and Disease Control Directorate, Ministry of Health, Morocco
[16] Blantyre Institute for Community Outreach, Malawi
[17] Federal Ministry of Health, Addis Ababa, Ethiopia
[18] Johns Hopkins School of Medicine, Ophthalmology Department, Baltimore, USA, 21287
[19] Amhara Public Health Institute, Bahir-Dar, Ethiopia

* Corresponding Author:
Benjamin F. Arnold, PhD
Associate Professor
F.I. Proctor Foundation
University of California, San Francisco
ben.arnold@ucsf.edu

Abstract

Trachoma, caused by ocular *Chlamydia trachomatis* infection, is targeted for global elimination as a public health problem by 2030. To provide evidence for use of antibodies to monitor *C. trachomatis* transmission, we collated IgG responses to Pgp3 antigen, PCR positivity, and clinical observations from 19,811 children aged 1–9 years in 14 populations. We demonstrate that age-seroprevalence curves consistently shift along a gradient of transmission intensity: rising steeply in populations with high levels of infection and active trachoma and becoming flat in populations near elimination. Seroprevalence (range: 0–54%) and seroconversion rates (range: 0–15 per 100 person-years) correlate with PCR prevalence (r: 0.88, 95% CI: 0.77, 0.93). A seroprevalence threshold of 13.5% (seroconversion rate 2.75 per 100 person-years) identifies clusters with any infection at high sensitivity (>90%) and moderate specificity (69-75%). Antibody responses in young children provide a robust, generalizable approach to monitor population progress toward and beyond trachoma elimination.

Introduction

Trachoma is the leading infectious cause of blindness and has been targeted for elimination as a public health problem by 2030.[1] Caused by repeated infections with the bacterium *Chlamydia trachomatis* (*Ct*), trachoma has historically been monitored via district-level estimates of clinical signs.[2] However, clinical signs may not align well with transmission intensity, particularly after mass drug administration of azithromycin (MDA) [3–5], and are prone to measurement error, especially as cases become rare.[6–8] As a result, there has been growing interest in IgG antibody responses as an objective and easy-to-collect biomarker to inform control programs. Based on examples from other infectious diseases including malaria [9] and SARS-CoV-2,[10] use cases for trachoma serology may include monitoring population-level transmission to determine appropriate interventions, post-validation surveillance, opportunistic investigation of populations using blood collected for other purposes, and fine-scale geographic targeting of control measures.[11–13]

IgG antibody responses to *Ct* antigens Pgp3 and CT694 are sensitive and specific markers of *Ct* infection.[14,15] Assays have demonstrated consistency across platforms (multiplex bead, enzyme-linked immunosorbent, lateral flow),[16,17] robust seropositivity cutoffs,[18] and high repeatability.[19] Of the two antigens, Pgp3 appears to elicit a stronger and more durable response and is collected in most trachoma serology surveys.[20] In epidemiologic studies, investigators have observed alignment between population-level summaries of antibody response and other trachoma markers, including the presence of *Ct* DNA, as determined by PCR, and the active trachoma sign trachomatous inflammation—follicular (TF). Individual studies suggest age-dependent

seroprevalence curves rise steeply with age among children in trachoma-endemic communities [14,15] and are flat in communities that have eliminated trachoma.[21–23] IgG responses to Pgp3 can be measured from dried blood spots and have the potential to be scaled through integration in multiplex surveillance strategies with other infectious pathogens.[24] Key next steps to advance the use of serology to monitor trachoma programs are to benchmark serology against independent measures of transmission, notably PCR, and to formalize the analytic approaches used to summarize trachoma antibody data.

Here, we collated IgG antibody, infection, and clinical data from 14 populations in five countries across a gradient of trachoma transmission intensities that ranged from hyper-endemic to post-elimination. Due to the shortcomings of clinical signs, we used PCR as the primary marker of trachoma activity, with TF as a secondary indicator to contextualize serological estimates. We hypothesized that population-level summaries of trachoma antibody measurements would follow a consistent path toward elimination, characterized by flattening of age-seroprevalence curves and a corresponding decline in seroconversion rates. We also hypothesized that different seroepidemiologic summary measures (e.g. seroprevalence, seroconversion rates) would be consistent with one another and align similarly with population-level transmission. We completed a series of analyses to test these hypotheses and in doing so, develop robust analytic methods for trachoma serology as we approach the elimination endgame.

Results

Study populations and settings

We compiled serological, molecular, and clinical measurements collected between 2012 and 2019 across nine studies in five countries (**Supplementary Table 1**) [4,25–32]. When possible, measurements within the same study were stratified into populations corresponding to trachoma evaluation units, resulting in 14 study populations. All studies were conducted in Africa and represented a gradient of trachoma transmission from hyper-endemic transmission to post-elimination. Measurements were taken at a single time point or annually with the exception of Dosso, Niger, where visits occurred every six months for the first year and annually thereafter. Due to changing transmission and/or interventions over time in some studies, analyses included only the most recent round of measurements for each population. We analyzed sampling clusters with 15 or more serological measurements, a total of 459 clusters. The median number of children contributing information per cluster was 40 (interquartile range: 32–48) (**Supplementary Fig. 1**), for a total of 19,811 serological measurements. Eleven studies included children aged 1–9 years, and three studies focused on children aged 1–5 years (**Supplementary Fig. 2**).

We generated population-level summaries using the median and range across clusters and observed wide variation in seroprevalence (median: 7%; range: 0–54%), PCR prevalence (median: 3%; range: 0–26%), and TF prevalence (median: 6%; range: 0–56%) (**Fig. 1**). PCR, a measure of current infection, may disappear rapidly following MDA [33]. Among clusters with MDA in the past year, the median PCR prevalence was 0%, while among clusters without recent MDA, PCR prevalence was 12%. Cluster-level

estimates within the same population were often variable, likely a combination of heterogeneity in disease transmission and stochasticity due to smaller sample sizes. Across the gradient of transmission intensities, population-level summaries of seroprevalence aligned with PCR and TF prevalence (**Fig. 1**).

Charting progress toward elimination using age-structured seroprevalence and seroconversion rates

We estimated age-dependent seroprevalence curves using semiparametric splines and seroconversion rates from age-structured seroprevalence (Methods). Across populations, seroconversion rates ranged from 0 to 15 per 100 person-years (median: 1.7) using a catalytic model without seroreversion (**Fig. 2**). Consistent with our hypothesis, we observed that age-seroprevalence curves were flatter and seroconversion rates were lower in areas with lower PCR prevalence. Age-seroprevalence curves rose steeply in settings with high levels of infection such as Wag Hemra and Andabet, Ethiopia, reaching >50% seroprevalence by age 9 years. In contrast, in populations with flatter curves (<10% seroprevalence by age 9 years, seroconversion rate <1 per 100 person-years), PCR prevalence was 0% when measured (Woreta town and Alefa, Ethiopia). Among populations with moderately increasing age-seroprevalence curves, roughly corresponding to seroconversion rates between 1 and 5 per 100 person-years, PCR prevalence ranged from 0 (Dera, Ethiopia) to 1.9% (Kongwa, Tanzania 2018).

Agreement between serology-based summary measures

Summary statistics estimated from age-seroprevalence curves provide additional, useful summary measures of transmission.[9,34] Population-level summaries of IgG responses include geometric mean IgG levels, seroprevalence, and seroconversion rates — each progression from IgG levels to seroconversion rates relies on additional model assumptions and analysis complexity (details in Methods). In the estimation of seroconversion rates from age-structured seroprevalence, we considered a range of model complexity that included a catalytic model (corresponding to a susceptible-infected-recovered, SIR, model), a reversible catalytic model allowing for seroreversion (corresponding to a susceptible-infected-susceptible, SIS, model), and a semiparametric hazard model that allowed for age-varying seroconversion rates.

A key question for elimination programs is whether the additional complexity in analysis leads to more useful information for identifying populations with ongoing ocular *Ct* transmission. We estimated each summary at the sampling cluster and population levels across the 14 study populations and found high correlation between all measures (Spearman $\rho \geq 0.88$ for all comparisons, **Fig. 3**). Cluster-level seroprevalence was strongly, linearly related with geometric mean IgG levels on the $\log_{10}$ scale (**Fig. 3a**), and there was a strong, non-linear relationship between seroprevalence and the seroconversion rate (**Fig. 3b**). Catalytic models that allowed for seroreversion shifted seroconversion rates up, particularly for clusters with a seroconversion rate greater than 20 per 100 person-years but had minimal influence on estimates at intermediate and lower levels of transmission (**Fig. 3c**). Similarly, seroprevalence was tightly linked with seroconversion rates that allowed for seroreversion in settings with lower prevalence,

and greater dispersion was observed in hyperendemic populations (**Fig. 3d**). The most complex model, a semiparametric proportional hazards spline model that allowed for an age-varying seroconversion rate, required more data than would be typically available at the sampling cluster level and thus could only be estimated at the population level where its estimates aligned closely with a simpler, constant rate model (**Supplementary Fig. 3**). These results show that all serologic summary measures provide similar information when averaged at the cluster or population level across all ranges of transmission and particularly at lower levels of transmission.

Comparing trachoma indicators in the presence and absence of MDA

As most trachoma program interventions act to clear infection or reduce its transmission, we sought summaries that could capture variation in populations' *Ct* infection burden. Seroprevalence and PCR prevalence aligned closely at the population level (r = 0.88; 95% CI: 0.77–0.93, **Fig. 4a**). At both the cluster- and population-levels, seroprevalence was almost always greater than or equal to PCR prevalence, underscoring the sensitivity of seroprevalence as a measure of current or past infection. However, PCR prevalence was highly variable across levels of seroprevalence; low PCR prevalence in the context of high seroprevalence may imply previously high levels of infection that had been controlled by MDA or other interventions. Relationships between TF and PCR prevalence were similar (population-level r = 0.92; 95% CI: 0.73–0.96, **Fig. 4b**).

As shown in prior work,[35] TF and seroprevalence were more strongly correlated with PCR prevalence in the absence of MDA in the past year (**Fig. 4a, 4b**). In the

absence of MDA, the relationship between seroprevalence and PCR prevalence was nearly linear, particularly in high transmission settings. In the presence of recent MDA, correlations between trachoma indicators weakened presumably because IgG and TF prevalence remain elevated as durable indicators of trachoma even after infections have been reduced through MDA.

We also stratified the analyses by child age and observed similar correlations between indicators among children aged 1–9 years compared to children aged 1–5 years (**Fig. 5**). When summarizing IgG responses as seroconversion rate instead of seroprevalence, overall results and subgroup results by recent MDA and age group were similar (**Supplementary Fig. 4**), reflecting the tight correlation between serologic summaries (**Fig. 3**). Our results show that serologic summaries align with PCR prevalence as well or better than TF, the current programmatic indicator, and that serology performs well even among preschool aged children. In populations that have recently undergone MDA, IgG and TF will likely remain elevated even as infection prevalence falls.

Assessing serologic thresholds for elimination of infections

Due to the wide variability in trachoma indicators both within and between populations, we used a nonparametric approach to evaluate potential serologic summary thresholds. Based on the alignment between seroprevalence and PCR at the cluster level and the relatively large number of clusters, we assessed sensitivity and specificity using cluster-level values. At each potential threshold, sensitivity and specificity were calculated across the 281 clusters with PCR measurements, 99 of

which had at least one infection detected by PCR. Although presence of a single infection is a stringent threshold, an appropriate level of PCR prevalence required to prevent blindness due to trachoma has yet to be established. Under this definition, a threshold with high sensitivity would result in more infected clusters being detected, while a threshold with high specificity might imply less unnecessary intervention. While overtreatment should be avoided, we focused on thresholds with high sensitivity with the goal of elimination in mind.

There was good classification of clusters with and without Ct infections based on either seroprevalence or seroconversion rates (AUC=0.92). Thresholds of 13.5% seroprevalence (**Fig. 6, Supplementary Table 2**) or 2.75 seroconversions per 100 person-years (**Supplementary Fig. 5, Supplementary Table 3**) had 90% sensitivity and 69-75% specificity to identify clusters with any PCR-detected infections. Thresholds of 22.5% seroprevalence and 5.75 seroconversions per 100 person-years had 80% sensitivity and 92-93% specificity. Thresholds were conservative when compared against population-specific sensitivity estimates in high transmission settings, but sensitivity dropped quickly in populations with very few infected clusters (n=4 in Chikwawa, Malawi and n=6 in Mchinji, Malawi) (**Fig. 6a**).

The overall analysis included all clusters regardless of age group. In a sensitivity analysis that included only children aged 1–5 years, classification of clusters with and without *Ct* infections was almost identical to the main analysis (AUC=0.92), and thresholds of 12.5% seroprevalence and 2.75 conversions per 100 person-years had 90% sensitivity and 69-71% specificity to identify clusters with any PCR-detected infections (**Supplementary Fig 6, Supplementary Table 4, Supplementary Table 5**).

In a supplementary assessment of the thresholds, we applied them to populations with very low trachoma prevalence that were not included in the threshold analysis because cluster-level PCR results were unavailable (Dosso, Alefa, and Woreta town, see **Figs. 1** and **2**). District-level PCR from Alefa and Woreta town were estimated to be 0%, and a recent study from the same population in Dosso found no *Ct* in pooled metagenomic testing of ocular swabs.[36] In these three populations, 98% of clusters (60/61) fell below the serologic thresholds for 90% sensitivity, supporting the interpretation of low levels of infection below the estimated thresholds.

Discussion

Using antibody measurements from 14 populations across a gradient of *Ct* transmission intensity, we demonstrated that IgG Pgp3 age-seroprevalence curves flatten and seroprevalence and seroconversion rates progress toward zero as populations approach elimination, consistent with biological assumptions and observations across other pathogens.[34,37] To our knowledge, this is the largest synthesis of *Ct* serology and infection data spanning globally relevant transmission settings from hyper-endemic to elimination. Summaries of IgG responses to *Ct* antigen Pgp3 among children aged 1–9 years aligned similarly with PCR prevalence and with one another at both the cluster- and population-levels, indicating that cluster-level Pgp3 summaries reflect variation in *Ct* infections and ongoing transmission. Combining information across all populations, we found that thresholds of 13.5% seroprevalence and 2.75 seroconversions per 100 person-years identified clusters with any infection with high sensitivity (>90%) and moderate specificity (69 to 75%). We observed similar results

when analyses were restricted to children aged 1–5 years, an age group that is potentially easier to sample in household surveys as they are not yet in school.

We demonstrated that seroprevalence and seroconversion rates perform as well or better as correlates of population levels of infection compared with clinical TF, and serology is arguably more objective, granular, and scalable for surveillance. Although clinical signs are important markers of disease progression, MDA is targeted towards *Ct* infections — if clinical signs continue to be present in the absence of antibody responses, further investigation may be warranted to determine other potential causes of inflammation. Compared to PCR, which also measures *Ct* infections, serology is cost-effective, with simpler collection procedures and the opportunity to leverage banked samples, and measures exposure over time versus at a single point, an advantage in low prevalence settings.

By focusing on parsimonious, generalizable methods, our aim was to present seroepidemiologic approaches that could be easily applied and interpreted by trachoma control programs. Trachoma programs currently rely on district-level estimates of active trachoma, and this analysis may be extended to develop district-level thresholds as an increasing number of district-level, population-based serological surveys become available. Cluster-level estimates, as investigated here, may be a promising alternative to identify focal areas for intervention, particularly in combination with geostatistical methods to improve precision and project across unsurveyed regions.[38]

Programmatic decisions related to suspension or reinitiation of antibiotic MDA primarily take place in low to intermediate transmission settings, and this study demonstrates that the information serologic surveillance provides in such settings

should be robust to choice of summary statistic. Serological summaries of increasing complexity were tightly correlated with one another, and the relationship was nearly linear in settings with low to intermediate transmission **(Fig. 3**). Quantitative IgG responses potentially provide information at very low levels of *Ct* transmission when most children are seronegative,[39] but a challenge is that IgG responses are in arbitrary units that may not be directly comparable across studies. Members of our team are developing a chimeric, monoclonal antibody to help facilitate direct comparison of quantitative antibody levels across studies.[12] Seroprevalence and seroconversion rates are standard transformations of the quantitative IgG response that are easier to compare across studies and labs. A potential drawback of seroprevalence and seroconversion is that they may be sensitive to choice of the seropositivity cutoff, potentially affecting programmatic decisions based on thresholds. In a sensitivity analysis, we found that identification of clusters with *Ct* infection based on seroprevalence and seroconversion rates were robust to large changes in the seropositivity cutoff (**Supplementary Fig 7**). The seroconversion rate is tightly linked to the slope of the age-seroprevalence curve (details in Methods). Additionally, the seroconversion rate implicitly adjusts for age (not guaranteed with mean IgG or seroprevalence) and can be interpreted as a measure of a pathogen's force of infection. Although we did not consider complicated seroconversion models that allowed for changes in transmission over time, such complexity may be less relevant when analyzing measurements from young children because their antibody responses reflect recent infections.[40–42] Our results support estimation of age-seroprevalence curves among young children combined with estimation of seroconversion rates using a simple,

single-rate model to characterize trachoma transmission. Our findings demonstrate that the slope of the age-seroprevalence curve and the seroconversion rate are sensitive and moderately specific markers of population-level *Ct* infection. Seroprevalence is another simple, robust summary measure that aligned with infections as well as seroconversion rate, particularly in the absence of recent MDA, but care should be taken to ensure similar age structure between populations to avoid bias.

We found that serologic summaries were sensitive indicators of *Ct* infection but have only moderate specificity: antibody responses were nearly always present in populations with infections, but the IgG signal persisted even if recent MDA reduced infection to low levels. This pattern suggests that populations requiring treatment will rarely be missed by serology but further verification with PCR could prevent overtreatment in the case of false positives. Because IgG responses to Pgp3 are durable, age-seroprevalence curves and statistics estimated from them may reflect historical transmission patterns and remain high despite low levels of infection resulting from control measures or secular trends. Restricting analysis to younger children (e.g., children born after discontinuing antibiotic MDA) or carefully accounting for past MDA treatments in the interpretation of antibody data may decrease false positives detected by IgG. At the cluster level, infections may also be missed due to small sample sizes. Extending this work using a freedom-from-infection framework may inform appropriate cluster-level sample sizes for a desired level of uncertainty.[43]

Here, we focused on IgG among young children and its relationship with *Ct* infection to extend a previous study that combined nine trachoma serology surveys and compared IgG seroconversion rates with clinical indicators among people of all ages.[40]

A focus on young children rather than all ages enabled us to simplify the modeling approach used to estimate seroconversion rates under the assumption that transmission was approximately stable over the age range. We focused on the relationship between serology and PCR infection to assess the utility of serology to monitor differences in pathogen transmission. The earlier synthesis compared indicators at the district level, which is the current scale of decision making for elimination programs. A caveat of the approach used in this study to identify serology thresholds to identify the presence of *Ct* infections is that we used clusters as the unit of analysis — a much finer spatial scale than district. We felt a similar, non-parametric threshold analysis at the district (study) level would not be informative with only 11 studies that included *Ct* infection measurements (**Fig. 1**), versus 281 unique clusters (**Fig. 6**). Future estimates of district-level serology thresholds for elimination, using the same summary statistics but potentially using a different approach to identify thresholds, would be a useful extension.

This work is subject to limitations. First, the data we analyzed were compiled from different previously published studies and sites that were available to us. Our results may not be representative of all populations with ongoing trachoma transmission. For example, the included studies come from five countries in Africa, but trachoma continues to be endemic in the other regions of Africa, Latin America, Asia, and the Pacific Islands.[44] As a secondary analysis, our work was also affected by design features of individual studies, such as site selection in RCTs, which were typically not selected using probability samples. Second, all models used to estimate seroconversion, except for the semiparametric spline model, assumed homogeneity of

seroconversion rate over age and time. For most studies, we expected stable transmission among 1–9-year-olds in the recent past. Our analysis used an estimate of seroreversion from one longitudinal cohort,[45] but data beyond this cohort is limited; however, based on a sensitivity analysis, no single seroreversion value resulted in the best model fit across populations (**Supplementary Fig. 8**). Finally, we were unable to evaluate more specific subgroups, such as populations with different MDA histories or populations experiencing recrudescence, due to limited data. Based on the variability observed between populations, refinement of thresholds may be warranted as more data are collected.

In conclusion, IgG responses to *Ct* antigen Pgp3 among 1–9-year-olds aligned closely with ongoing transmission as measured by PCR and TF across a range of trachoma endemicity settings. Consistent with patterns observed across other pathogens, age-dependent Pgp3 seroprevalence curves became flatter and seroconversion rates declined to zero as populations approached elimination — providing a coherent framework for monitoring *Ct* transmission in seroepidemiologic studies. Serologic summaries estimated via a range of model complexity were sensitive markers of ocular chlamydial infection and were consistent with one another, implying that simpler approaches are likely sufficient to capture variation in transmission. These results support use of serologic surveys to inform trachoma programs as populations approach elimination.

Methods

Contributing studies

We gathered data from published trachoma serology surveys, with an emphasis on IgG antibody responses to Pgp3 collected among children aged 1–9 years and relatively recent reports (**Supplementary Table 1**). All studies were conducted between 2012 and 2019. Children below the age of 1 year were excluded to mitigate the influence of maternal antibodies. Based on the original study designs, measurements in Matameye, Niger (PRET) and Wag Hemra, Ethiopia (TAITU) were restricted to children aged under 6 years; in Dosso, Niger (MORDOR), the study was limited to children aged under 5 years; and in Alefa, Andabet, Dera, and Woreta town, Ethiopia, infections were measured among children aged 1–5-years, while serology and TF were measured among children aged 1–9-year. For measurements collected as part of a population-based surveys, multi-level cluster random sampling was used. For measurements collected as part of a randomized controlled trial, we combined data across arms unless otherwise noted (e.g., stratification by recent MDA). Due to changing transmission and/or control interventions in studies with repeated cross-sectional data (WUHA in Wag Hemra, Ethiopia; Kongwa, Tanzania from 2012-2015; MORDOR in Dosso, Niger), we included only the most recent year of measurements with serology, and PCR measurements if available, for each population. We excluded clusters with fewer than 15 children measured to ensure sufficient information to estimate cluster level means (n=22 clusters excluded, reduced from 481 to 459).

Details of serological, clinical, and PCR measurements can be found in the published reports for each study [4,25–32]. In all but one study, dried blood spots were

analyzed for IgG antibodies to Pgp3 using a multiplex bead assay on a Luminex platform and were reported as median fluorescence intensity minus background (MFI-bg), and seropositivity cutoffs were generated using receiver operator characteristic (ROC) methods [14]. In Malawi, dried blood spots were tested for IgG antibodies against Pgp3 using ELISA, and the seropositivity cutoff was determined based on a finite mixture model [31]. ELISA-based population-level measurements of Pgp3 have been shown to have good agreement with multiplex bead assays [46]. We used cutoffs defined by each study to assign seropositivity status. To assess robustness to seropositivity cutoffs, we compared seroprevalence and seroconversion rate calculated across a range of arbitrary cutoffs for four study populations at different levels of trachoma prevalence (**Supplementary Fig. 7**). Clinical disease was assessed by trained field graders according to the WHO simplified grading system [47], which defines TF as the presence of five or more follicles which are (a) at least 0.5 mm in diameter and (b) located in the central part of the upper tarsal conjunctiva. Conjunctival swabs were assessed for *Ct* DNA using PCR. In 5 out of 7 studies with PCR measurements, cluster-level prevalence was estimated from individual-level results [29–31,48,49]; in one study (PRET), cluster-level prevalence was estimated from pooled results using maximum likelihood methods [50,51]. For Andabet, Dera, Woreta town, and Alefa, Ethiopia, *Ct* infection prevalence was estimated at the district level from pooled results using maximum likelihood methods [26].

Cluster-level prevalence was calculated as the number of children who were sero-, PCR- or TF-positive divided by the number of children tested for the respective outcome. When possible, “populations” were defined by districts or evaluation units

currently used for trachoma monitoring. Population-level prevalence estimates were defined as the median value across clusters. Age-seroprevalence curves were estimated by pooling all measurements at the population level, calculating seroprevalence for one-year age groups, and fitting cubic spline models to generate smooth trend lines.

Estimating serology-based summary measures

We summarized IgG responses as geometric mean IgG levels, seroprevalence, and seroconversion rates from several models. The seroconversion rate from a current status, single-rate catalytic model assuming no seroreversion is closely tied to the slope of age-seroprevalence curve.[52] Specifically, the hazard (seroconversion rate) is equal to the slope of the age-seroprevalence curve divided by the complement of the seroprevalence at age a. It can be shown that the seroconversion rate based on this model can be estimated as the exponentiated intercept from a generalized linear model with binomial error structure and a complementary log-log link: [53]

$$\log\left[-\log\left(1 - P(Y = 1 \mid A)\right)\right] = \log(\lambda) + \log(A)$$

where Y represents individual level serostatus (1: seropositive, 0: seronegative or equivocal), A is the child's age in years, and λ is the seroconversion rate. The seroconversion rate provides an estimate of the force of infection, an epidemiological parameter that denotes the rate at which susceptible individuals in the population become infected.

Next, we extended this model to allow for seroreversion. Cross-sectional data do not contain sufficient information to reliably estimate both seroreversion and

seroconversion rates.[54] Therefore, we fit a binomial maximum likelihood model for seroconversion with fixed seroreversion rates ranging from 0.02 to 0.20 per person-year:[21,26,40]

$$P(Y = 1 \mid A) = \frac{\lambda}{\lambda + \rho}[1 - \exp(-(\lambda + \rho) \times A)]$$

where ρ is the assumed seroreversion rate. In our main analyses, we assumed a seroreversion rate of 6.6 per 100 person-years based on a longitudinal cohort in Kongwa, Tanzania monitored in the absence of MDA [45], which is likely conservative for higher transmission settings. No level of seroreversion consistently provided the best fit across populations (**Supplementary Fig. 8**). This model did not converge in several clusters (6 out of 416 clusters with seroprevalence >0%, or 1.4%), which often contained few seropositive children.

Finally, we fit semiparametric spline models to allow seroconversion to vary by age.[52] We fit this model only at the population level, as it requires more data than are typically available at the sampling cluster level (around 20-40 children). We fit a generalized linear model with complementary log-log link for seropositivity:

$$\log\left[-\log\left(1 - P(Y = 1 \mid A)\right)\right] = g(A)$$

where *g(A)* is a flexible function for age modeled using cubic splines. To estimate the average seroconversion rate in each population, λ, we integrated over age using predictions from the model. We used the relationship between the hazard $\lambda(a)$ and cumulative incidence $F(a)$, where $F(a)$ is the predicted seroprevalence at age a (details in [37]).

$$\lambda = \int_{a_1}^{a_2} \lambda(a)da = \frac{\log[1 - F(a_1)] - \log[1 - F(a_2)]}{a_2 - a_1}$$

471

472 **Comparison of different trachoma indicators**

473 We used the Pearson correlation coefficient to compare serologic summaries
474 and TF prevalence with PCR prevalence at the population and cluster levels. We
475 conducted this analysis across all populations with PCR measurements and explored
476 the impact of contextual factors by stratifying clusters into subgroups defined by MDA in
477 the past year (yes / no) and age range (1–9-year-olds / 1–5-year-olds).

478 We used the Spearman rank correlation coefficient to compare different serologic
479 summaries with one another at the cluster level, allowing for non-linearity in the
480 relationships. We estimated simultaneous confidence intervals from a cubic spline to
481 summarize the relationship between markers at the cluster level, including a random
482 effect for study to allow for correlated measures within-study.

483

484 **Serologic thresholds for elimination**

485 We used a non-parametric approach to assess thresholds of seroprevalence or
486 seroconversion rates to classify clusters without PCR infections. For overall estimates,
487 we combined clusters from all populations with PCR measurements, for a total of 281
488 clusters and 99 clusters with at least one PCR-detected infection. We defined a range of
489 cutoffs covering nearly all cluster-level estimates (0 to 100% for seroprevalence, 0 to 50
490 per 100 person-years for seroconversion rate) and divided the range into 200
491 increments. At each step, we calculated sensitivity as the proportion of clusters with
492 serology values above the threshold among clusters with any infection, and specificity
493 as the proportion of clusters with serology value less than or equal to the threshold

among clusters with zero infections detected. We identified the highest thresholds achieving at least 90% and 80% sensitivity. We also presented these results as receiver operating characteristic (ROC) curves and calculated overall area-under-the-curve (AUC). We calculated sensitivity, specificity, and the ROC curve for each population separately.

Data availability

R version 4.2.2 (2022-10-21, “Innocent and Trusting”) was used for this analysis.[55] De-identified data and all code to reproduce this work are publicly available (*note: during peer review we are finalizing agreements to provide de-identified data*): https://osf.io/e6j5a/ .

Acknowledgements

Ethics statement. The secondary analysis protocol was reviewed and approved by the Institutional Review Board at the University of California, San Francisco (Protocol #20-33198). All primary data that contributed to the analysis was collected after obtaining informed consent from all participants or their guardians under separate human subjects research protocols in accordance with the Declaration of Helsinki.

Conflict of interest statement. The authors have no conflicts of interest to report. The authors alone are responsible for the views expressed in this article, and they do not necessarily represent the views, decisions, or policies of the institutions with which they are affiliated.

Funding statement. This work was supported by the National Institute of Allergy and Infectious Diseases (R01-AI158884 to B.F.A.). AWS is a staff member of the World Health Organization.

Disclaimer. The findings and conclusions in this article are those of the authors and do not necessarily represent the official position of the National Institutes of Health or the Centers for Disease Control and Prevention. Use of trade names is for identification only and does not imply endorsement by the Public Health Service or by the U.S. Department of Health and Human Services.

Author contributions (CRediT taxonomy).
Conceptualization: CT, AWS, DLM, SDN, PJL, BFA
Data curation: CT, DLM, BFA
Formal analysis: CT, BFA
Funding acquisition: BFA, DLM
Investigation: CT, BFA
Methodology: CT, BFA
Project administration: DLM, BFA
Resources: All authors
Software: CT, BFA
Supervision: AWS, DLM, SDN, SKW, TML, JDK, PJL
Validation: CT, BG, DLM, BFA
Visualization: CT, BFA
Writing - original draft preparation: CT, BFA
Writing - review & editing: All authors

References

1. World Health Organization. *Ending the neglect to attain the sustainable development goals: a roadmap for neglected tropical diseases 2021-2030.* https://apps.who.int/iris/handle/10665/361856 (2020).
2. Taylor, H. R., Burton, M. J., Haddad, D., West, S. & Wright, H. Trachoma. *The Lancet* **384**, 2142–2152 (2014).
3. Keenan, J. D. *et al.* Clinical Activity and Polymerase Chain Reaction Evidence of Chlamydial Infection after Repeated Mass Antibiotic Treatments for Trachoma. *Am. J. Trop. Med. Hyg.* **82**, 482–487 (2010).
4. Amza, A. *et al.* Community-level Association between Clinical Trachoma and Ocular Chlamydia Infection after MASS Azithromycin Distribution in a Mesoendemic Region of Niger. *Ophthalmic Epidemiol.* **26**, 231–237 (2019).
5. Ramadhani, A. M., Derrick, T., Macleod, D., Holland, M. J. & Burton, M. J. The Relationship between Active Trachoma and Ocular Chlamydia trachomatis Infection before and after Mass Antibiotic Treatment. *PLoS Negl. Trop. Dis.* **10**, e0005080 (2016).
6. Assaad, F. A. & Maxwell-Lyons, F. Systematic observer variation in trachoma studies. *Bull. World Health Organ.* **36**, 885–900 (1967).
7. Tielsch, J. M. *et al.* Trachoma grading: observer trials conducted in southern Malawi. *Br. J. Ophthalmol.* **71**, 371–374 (1987).
8. Gebresillasie, S. *et al.* Inter-Rater Agreement between Trachoma Graders: Comparison of Grades Given in Field Conditions versus Grades from Photographic Review. *Ophthalmic Epidemiol.* **22**, 162–169 (2015).
9. Corran, P., Coleman, P., Riley, E. & Drakeley, C. Serology: a robust indicator of malaria transmission intensity? *Trends Parasitol.* **23**, 575–582 (2007).
10. Stringhini, S. *et al.* Seroprevalence of anti-SARS-CoV-2 IgG antibodies in Geneva, Switzerland (SEROCoV-POP): a population-based study. *Lancet Lond. Engl.* **396**, 313–319 (2020).
11. Woodhall, S. C. *et al.* Advancing the public health applications of Chlamydia trachomatis serology. *Lancet Infect. Dis.* **18**, e399–e407 (2018).
12. Martin, D. L. *et al.* The use of serology for trachoma surveillance: Current status and priorities for future investigation. *PLoS Negl. Trop. Dis.* **14**, e0008316 (2020).
13. Cooley, G. M. *et al.* No Serological Evidence of Trachoma or Yaws Among Residents of Registered Camps and Makeshift Settlements in Cox's Bazar, Bangladesh. *Am. J. Trop. Med. Hyg.* **104**, 2031–2037 (2021).
14. Goodhew, E. B. *et al.* CT694 and pgp3 as Serological Tools for Monitoring Trachoma Programs. *PLoS Negl. Trop. Dis.* **6**, e1873 (2012).
15. Goodhew, E. B. *et al.* Longitudinal analysis of antibody responses to trachoma antigens before and after mass drug administration. *BMC Infect. Dis.* **14**, 3154 (2014).
16. Gwyn, S. *et al.* Comparison of Platforms for Testing Antibody Responses against the Chlamydia trachomatis Antigen Pgp3. *Am. J. Trop. Med. Hyg.* **97**, 1662–1668 (2017).
17. Wiegand, R. E. *et al.* Latent class modeling to compare testing platforms for detection of antibodies against the Chlamydia trachomatis antigen Pgp3. *Sci. Rep.* **8**, 4232 (2018).
18. Migchelsen, S. J. *et al.* Defining Seropositivity Thresholds for Use in Trachoma Elimination Studies. *PLoS Negl. Trop. Dis.* **11**, e0005230 (2017).
19. Kaur, H., Dize, L., Munoz, B., Gaydos, C. & West, S. K. Evaluation of the reproducibility of a serological test for antibodies to Chlamydia trachomatis pgp3: A potential surveillance tool for trachoma programs. *J. Microbiol. Methods* **147**, 56–58 (2018).

20. Wang, J. *et al.* A Genome-Wide Profiling of the Humoral Immune Response to Chlamydia trachomatis Infection Reveals Vaccine Candidate Antigens Expressed in Humans. *J. Immunol.* **185**, 1670–1680 (2010).
21. Martin, D. L. *et al.* Serology for Trachoma Surveillance after Cessation of Mass Drug Administration. *PLoS Negl. Trop. Dis.* **9**, e0003555 (2015).
22. Pant, B. P. *et al.* Control of Trachoma from Achham District, Nepal: A Cross-Sectional Study from the Nepal National Trachoma Program. *PLoS Negl. Trop. Dis.* **10**, e0004462 (2016).
23. West, S. K. *et al.* Can We Use Antibodies to Chlamydia trachomatis as a Surveillance Tool for National Trachoma Control Programs? Results from a District Survey. *PLoS Negl. Trop. Dis.* **10**, e0004352 (2016).
24. Arnold, B. F., Scobie, H. M., Priest, J. W. & Lammie, P. J. Integrated Serologic Surveillance of Population Immunity and Disease Transmission. *Emerg. Infect. Dis.* **24**, 1188–1194 (2018).
25. Kim, J. S. *et al.* Community-level chlamydial serology for assessing trachoma elimination in trachoma-endemic Niger. *PLoS Negl. Trop. Dis.* **13**, (2019).
26. Nash, S. D. *et al.* Population-Based Prevalence of Chlamydia trachomatis Infection and Antibodies in four Districts with Varying Levels of Trachoma Endemicity in Amhara, Ethiopia. *Am. J. Trop. Med. Hyg.* (2020) doi:10.4269/ajtmh.20-0777.
27. Wittberg, D. M. *et al.* WASH Upgrades for Health in Amhara (WUHA): study protocol for a cluster-randomised trial in Ethiopia. *BMJ Open* **11**, e039529 (2021).
28. Keenan, J. D. *et al.* Azithromycin to Reduce Childhood Mortality in Sub-Saharan Africa. *N. Engl. J. Med.* **378**, 1583–1592 (2018).
29. Wilson, N. *et al.* Evaluation of a Single Dose of Azithromycin for Trachoma in Low-Prevalence Communities. *Ophthalmic Epidemiol.* **26**, 1–6 (2019).
30. Odonkor, M. *et al.* Serology, infection, and clinical trachoma as tools in prevalence surveys for re-emergence of trachoma in a formerly hyperendemic district. *PLoS Negl. Trop. Dis.* **15**, e0009343 (2021).
31. Burr, S. E. *et al.* Pgp3 seroprevalence and associations with active trachoma and ocular Chlamydia trachomatis infection in Malawi: cross-sectional surveys in six evaluation units. *PLoS Negl. Trop. Dis.* **13**, e0007749 (2019).
32. Hammou, J. *et al.* Post-Validation Survey in Two Districts of Morocco after the Elimination of Trachoma as a Public Health Problem. *Am. J. Trop. Med. Hyg.* **106**, 1370–1378 (2022).
33. Solomon, A. W. *et al.* Trachoma. *Nat. Rev. Dis. Primer* **8**, 1–20 (2022).
34. Arnold, B. F. *et al.* Measuring changes in transmission of neglected tropical diseases, malaria, and enteric pathogens from quantitative antibody levels. *PLoS Negl. Trop. Dis.* **11**, e0005616 (2017).
35. Tedijanto, C. *et al.* Predicting future community-level ocular Chlamydia trachomatis infection prevalence using serological, clinical, molecular, and geospatial data. *PLoS Negl. Trop. Dis.* **16**, e0010273 (2022).
36. Arzika, A. M. *et al.* Effect of Biannual Mass Azithromycin Distributions to Preschool-Aged Children on Trachoma Prevalence in Niger: A Cluster Randomized Clinical Trial. *JAMA Netw. Open* **5**, e2228244 (2022).
37. Arnold, B. F. *et al.* Fine-scale heterogeneity in *Schistosoma mansoni* force of infection measured through antibody response. *Proc. Natl. Acad. Sci.* **117**, 23174–23181 (2020).
38. Amoah, B. *et al.* Model-based geostatistics enables more precise estimates of neglected tropical-disease prevalence in elimination settings: mapping trachoma prevalence in Ethiopia. *Int. J. Epidemiol.* **51**, 468–478 (2022).
39. Arnold, B. F. *et al.* Measuring changes in transmission of neglected tropical diseases, malaria, and enteric pathogens from quantitative antibody levels. *PLoS Negl. Trop. Dis.* **11**, e0005616 (2017).

642 40. Pinsent, A. *et al.* The utility of serology for elimination surveillance of trachoma. *Nat. Commun.* **9**, 5444 (2018).
643
644 41. Yman, V. *et al.* Antibody acquisition models: A new tool for serological surveillance of malaria transmission intensity. *Sci. Rep.* **6**, 19472 (2016).
645
646 42. Sepúlveda, N., Stresman, G., White, M. T. & Drakeley, C. J. Current Mathematical Models for Analyzing Anti-Malarial Antibody Data with an Eye to Malaria Elimination and Eradication. *J. Immunol. Res.* **2015**, 1–21 (2015).
647
648
649 43. Michael, E. *et al.* Substantiating freedom from parasitic infection by combining transmission model predictions with disease surveys. *Nat. Commun.* **9**, 4324 (2018).
650
651 44. Renneker, K. K. *et al.* Global progress toward the elimination of active trachoma: an analysis of 38 countries. *Lancet Glob. Health* **10**, e491–e500 (2022).
652
653 45. West, S. K. *et al.* Longitudinal change in the serology of antibodies to Chlamydia trachomatis pgp3 in children residing in a trachoma area. *Sci. Rep.* **8**, 3520 (2018).
654
655 46. Gwyn, S. *et al.* The Performance of Immunoassays to Measure Antibodies to the Chlamydia trachomatis Antigen Pgp3 in Different Epidemiological Settings for Trachoma. *Am. J. Trop. Med. Hyg.* (2021) doi:10.4269/ajtmh.21-0541.
656
657
658 47. Thylefors, B., Dawson, C. R., Jones, B. R., West, S. K. & Taylor, H. R. A simple system for the assessment of trachoma and its complications. *Bull. World Health Organ.* **65**, 477–483 (1987).
659
660
661 48. Melo, J. S. *et al.* Targeted antibiotics for trachoma: a cluster-randomized trial. *Clin. Infect. Dis.* ciab193 (2021) doi:10.1093/cid/ciab193.
662
663 49. Aragie, S. *et al.* Water, sanitation, and hygiene for control of trachoma in Ethiopia (WUHA): a two-arm, parallel-group, cluster-randomised trial. *Lancet Glob. Health* **10**, e87–e95 (2022).
664
665 50. Ray, K. J. *et al.* Estimating Community Prevalence of Ocular *Chlamydia trachomatis* Infection using Pooled Polymerase Chain Reaction Testing. *Ophthalmic Epidemiol.* **21**, 86–91 (2014).
666
667
668 51. Amza, A. *et al.* A Cluster-Randomized Trial to Assess the Efficacy of Targeting Trachoma Treatment to Children. *Clin. Infect. Dis.* **64**, 743–750 (2017).
669
670 52. Hens, N., Shkedy, Z., Aerts, M., Damme, C. F. P. V. & Beutels, P. *Modeling Infectious Disease Parameters Based on Serological and Social Contact Data*. (Springer, 2012).
671
672 53. Jewell, N. P. & Laan, M. V. Generalizations of current status data with applications. *Lifetime Data Anal.* **1**, 101–109 (1995).
673
674 54. Arnold, B. F. *et al.* Enteropathogen antibody dynamics and force of infection among children in low-resource settings. *eLife* **8**, e45594 (2019).
675
676 55. R Core Team. *R: A language and environment for statistical computing.* (R Foundation for Statistical Computing, 2020).
677
678 56. Hammou, J. *et al.* In Morocco, the elimination of trachoma as a public health problem becomes a reality. *Lancet Glob. Health* **5**, e250–e251 (2017).
679
680

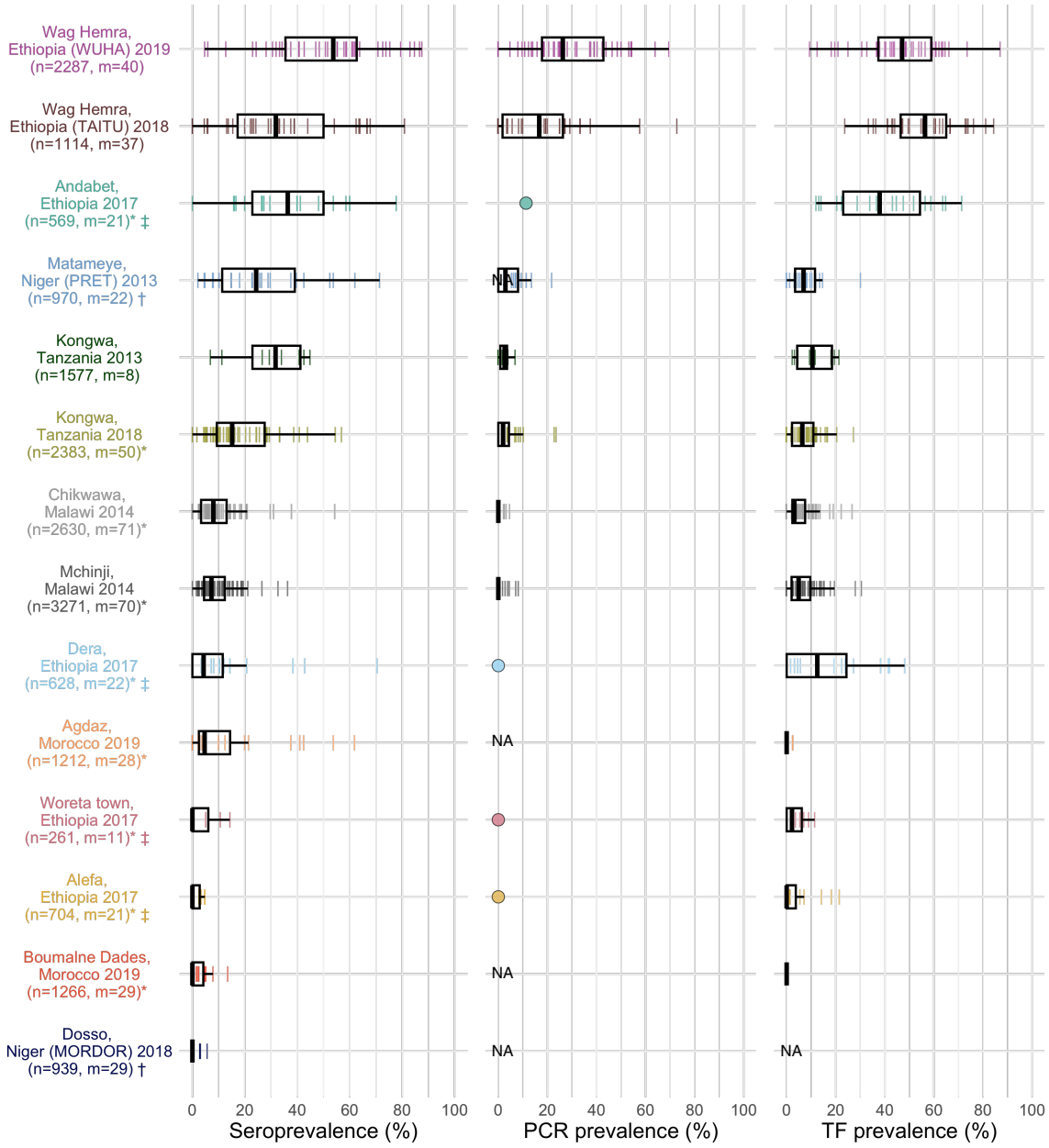

Abbreviations: n = number of individuals measured; m = number of clusters
* Estimates collected in population-based prevalence survey
† Serology, PCR, and TF measured among 1–5-year-olds
‡ PCR prevalence estimated only at district-level among 1–5-year-olds

Figure 1. Seroprevalence, PCR positivity, and TF prevalence across study populations. Cluster-level prevalence estimates are represented by colored lines, and overlaid boxplots show the median, interquartile range, and range (excluding outliers defined as points more than 1.5 times the interquartile range from the 25th or 75th percentile) for each population. Study site, country, study name (if applicable), and year of data collection are listed on the left with number of individuals (n) and number of clusters (m) included in the analyses. For studies with only district-level estimates of PCR prevalence the mean is indicated with a circle rather than box plot. NA marks studies that did not measure PCR or trachomatous inflammation—follicular (TF). Study populations are arranged in descending order of seroconversion rates, presented in Figure 2.

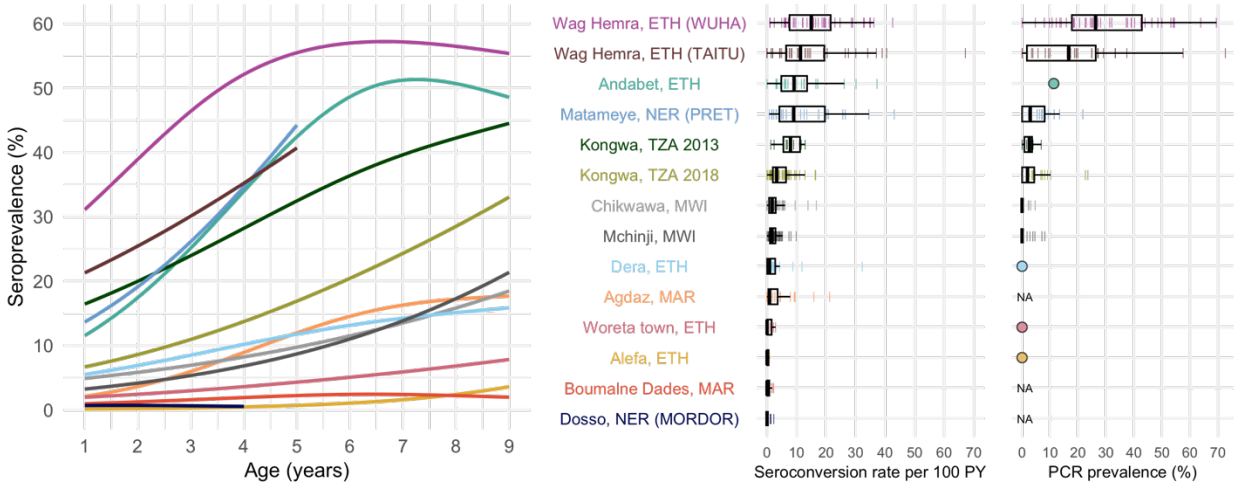

Abbreviations: PY = person-years; ETH = Ethiopia; NER = Niger; TZA = Tanzania; MWI = Malawi; MAR = Morocco

Figure 2. Age-dependent seroprevalence curves, modeled seroconversion rates, and PCR prevalence across study populations. Cubic splines fit to seroprevalence by age are shown in the left plot. Cluster-level seroconversion rates and PCR prevalence estimates are represented by colored lines, and overlaid boxplots show the median, interquartile range, and range excluding outliers for each population. Study populations are arranged in descending order of median seroconversion rate assuming no seroreversion. *Ct* PCR measurements are identical to Figure 1 and are included for reference. For studies with only district-level estimates of PCR prevalence the mean is indicated with a circle rather than box plot. NA indicates that a study did not measure *Ct* infections with PCR.

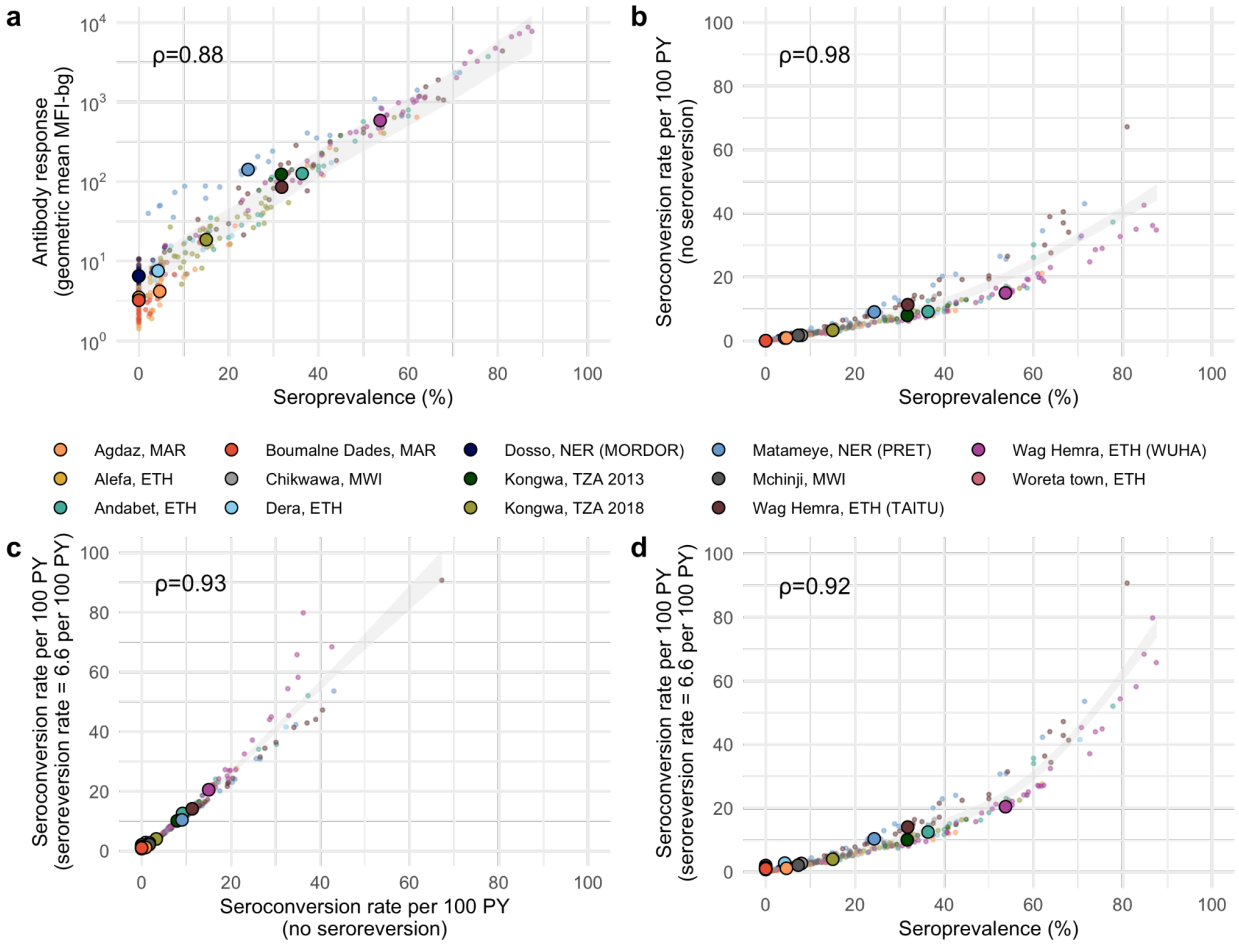

Figure 3. Relationship between different cluster-level summaries including geometric mean IgG response, seroprevalence, and seroconversion rates with and without seroreversion. Spearman rank correlations across sampling clusters (a-d) are shown for each comparison. A fixed seroreversion rate of 6.6 per 100 person-years was assumed in the catalytic model allowing for seroreversion (Methods). Shaded bands show simultaneous 95% confidence intervals for a spline fit through cluster-level estimates. Abbreviations: PY = person-years; ETH = Ethiopia; MAR = Morocco; MWI = Malawi; NER = Niger; TZA = Tanzania.

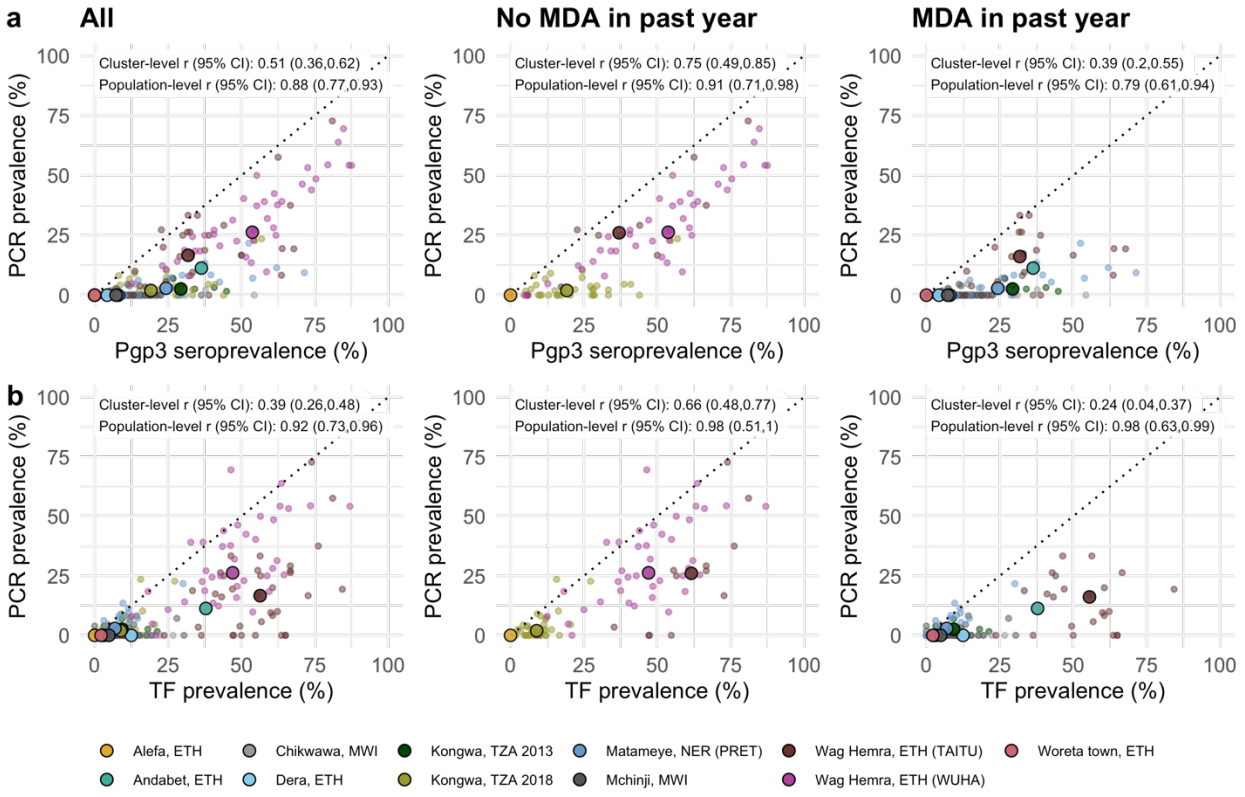

Figure 4. Relationship between trachoma biomarkers in the presence and absence of recent mass drug administration (MDA). a Correlations between cluster PCR prevalence and seroprevalence overall and stratified by whether the study population had received MDA in the previous year. b Correlations between PCR prevalence and TF prevalence overall and stratified by whether the study population had received MDA in the previous year. In all panels, medians across clusters for each study population are represented by larger points with black outline. Each plot includes the identity line (dotted) and Pearson correlations at the cluster- and population-levels. 95% confidence intervals (CIs) are based on 1,000 bootstrapped samples, holding populations fixed and resampling clusters with replacement. Population-level values are included for Andabet, Dera, Woreta town, and Alefa, Ethiopia, but cluster-level values were not available for these populations. Abbreviations: ETH = Ethiopia; MWI = Malawi; NER = Niger; TZA = Tanzania.

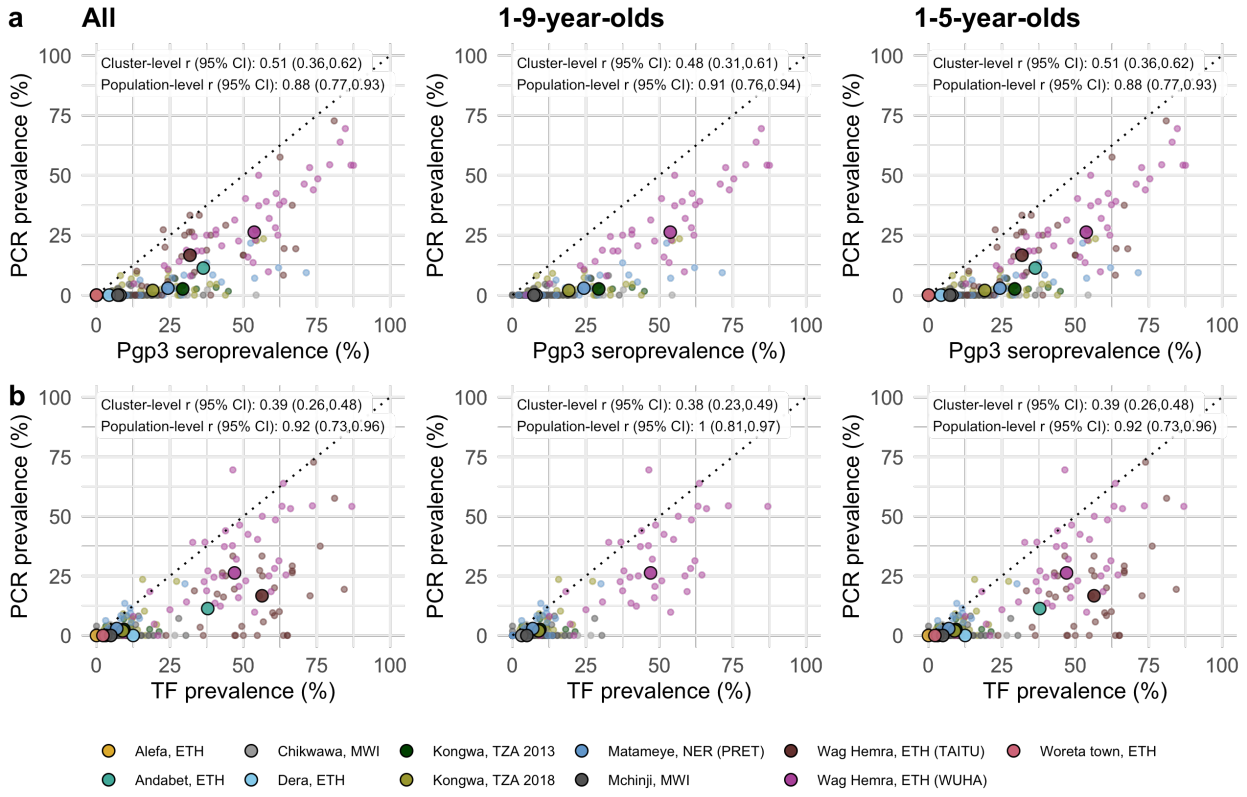

Figure 5. Relationship between trachoma biomarkers in different monitoring age ranges. **a** Correlations between cluster PCR prevalence and seroprevalence overall and stratified by age of monitoring population. **b** Correlations between PCR prevalence and TF prevalence overall and stratified by age of monitoring population. In all panels, medians across clusters for each study population are represented by larger points with black outline. Each plot includes the identity line (dotted) and Pearson correlations at the cluster- and population-levels. 95% confidence intervals (CIs) are based on 1,000 bootstrapped samples, holding populations fixed and resampling clusters with replacement. Population-level values are included for Andabet, Dera, Woreta town, and Alefa, Ethiopia, but cluster-level PCR prevalence was not available for these populations. Abbreviations: ETH = Ethiopia; MWI = Malawi; NER = Niger; TZA = Tanzania.

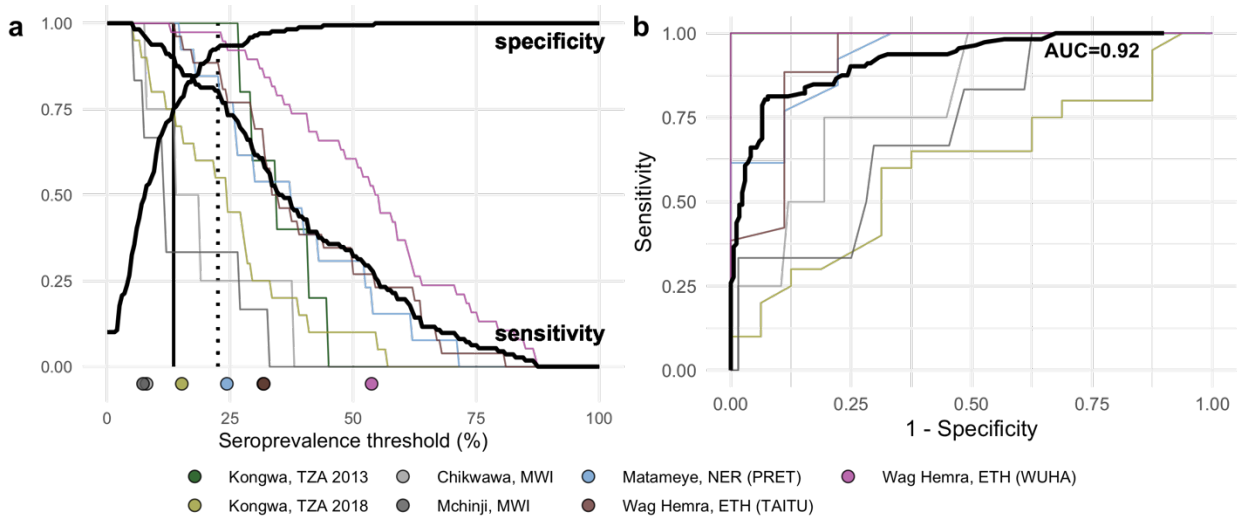

Abbreviations: ETH = Ethiopia; NER = Niger; TZA = Tanzania; MWI = Malawi

Figure 6. Identification of clusters with *C. trachomatis* infection using seroprevalence. (**a**) Sensitivity and specificity curves for identification of clusters with any *Ct* infections based on different seroprevalence thresholds among children 1-9 years old (n = 281 clusters, 99 clusters with PCR>0%). Vertical lines delineate sensitivity at 90% (solid line, 13.5% seroprevalence) and 80% (dotted line, 22.5% seroprevalence). Thin lines show sensitivity for each study population with cluster-level PCR measurements. Points at bottom of plot mark seroprevalence estimates for each study population. (**b**) Receiver operating characteristic (ROC) curves for all clusters (thick black line) and for each population (thin colored lines) with overall area-under-the-curve (AUC).